Experimental Results of a 1Mbps IR Transceiver for Indoor Wireless Local Area Networks

António M. R. Tavares*, Adriano J. C. Moreira, Cipriano R. A. T. Lomba, Luís M. V. Moreira, Rui J. M. T. Valadas, A. M. de Oliveira Duarte

Integrated Broadband Communications Group
Dept. of Electronics and Telecommunications
University of Aveiro
3800 AVEIRO
PORTUGAL
Tel: +351.34.381937
Fax: +351.34.381941
e-mail: tavares@zeus.ci.ua.pt

Abstract

This paper presents the design and implementation of an infrared transceiver prototype for Indoor Wireless Local Area Networks. The infrared transceiver prototype operates at *1Mbps* using Differential Manchester line coding. The system was designed to operate in completely diffuse environments.

A model for the theoretical sensitivity of the optical receiver is developed. The system design options are presented and discussed focusing on the characteristics of the optical noise sources, the electromagnetic interference and the optoelectronic devices. The transmitter prototype emits a Differential Manchester signal at a centre wavelength of *850nm* having an average optical power of about *400mW*. The receiver consists of a differential front-end using an array of PIN photodiodes with a total active area of $3.4cm^2$. A receiver sensitivity (minimum irradiance corresponding to a 10^{-9} bit error rate) of $-43.1dBm/cm^2$ was measured which is only *1.1dB* from the theoretical calculated sensitivity when only natural light was presented. It was demonstrated that the optical interference, induced by fluorescent lamps, introduces a large penalty in the receiver sensitivity.

This work is being carried out as part of the ESPRIT.6892 - POWER (Portable Workstation for Education in Europe) project commissioned by the European Commission.

* The first author would like to thank to JNICT (*Junta Nacional de Investigação Científica e Tecnológica*) for its financial support through a *Ph.D.* grant BD/2599/93.

I. Introduction

New requirements of computer users and the explosion of the portable computer market are pushing for the growth of indoor Wireless Local Area Networks (WLANs). Traditional computer networks use wires to exchange information. The costs of wires and installation procedures make wired networks less attractive than WLANs. For all these reasons, indoor WLANs have become an emerging issue of research and development [1-8].

The interest in indoor WLANs has evolved in two wireless technologies: radio frequency and infrared (IR). Since the communication medium is confined to closed spaces, IR technology has some advantages when compared to radio frequency. The main advantages of IR are the provision of broadband and its security: as it is confined to closed rooms, it does not interfere with systems in adjacent rooms. On the other hand, optical safety exposition limits, optical noise from natural and artificial lights [9], and multipath dispersion [7] are the main factors limiting the range and speed of IR based systems.

This paper focus on the IR technology associated to WLANs. The design and implementation of an IR transceiver prototype is presented. The IR transceiver prototype operates at *1Mbps* using Differential Manchester line coding. The system was designed to operate in a completely diffuse environment. An analysis of the optical transimpedance receiver sensitivity is performed. Experimental results of the transimpedance receiver operating at *1Mbps* are also included.

Section II presents general considerations about our indoor WLAN, the ambient light noise and the adopted encoding method. A description of the IR emitter and receiver is presented in section III. Section IV presents the evaluation of the theoretical receiver sensitivity. Section V presents experimental results and compares them with the values evaluated theoretically. Some tests in an indoor WLAN environment are reported in section VI. Finally, section VII presents the main conclusions of this work.

II. General Considerations

1. Indoor IR WLAN Description

A diffuse WLAN uses a large beam to illuminate a large portion of the ceiling and/or walls. The diffuse reflection is received by a detector with a large Field Of View (FOV). In the definition of our indoor WLAN we assume a diffuse configuration based on a passive reflection. The IR transceivers are aimed to ceiling.

The IR transceivers were designed to cover a circular communication cell with a radius of about *6m* (approximately $113m^2$). The physical configuration of the implemented system is presented in figure 1.

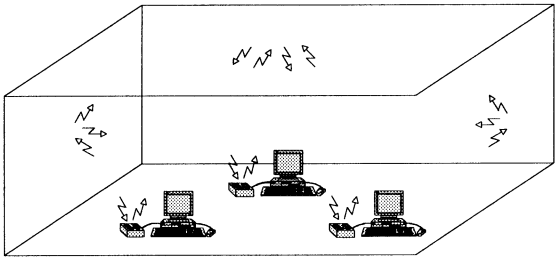

Figure 1. IR WLAN configuration.

2. Ambient Light Noise

There are a set of constraint factors which limit the performance of wireless optical systems. The most limitative are: i) the shot noise induced by ambient light due to natural and artificial light, ii) the interference induced by artificial light and iii) the large value of the parasitic capacitance of the receiving PIN photodiodes.

To evaluate the theoretical receiver sensitivity of the optical receiver, we have to take into account the *dc* photocurrent induced into the photodetector by the ambient light. The shot noise power is directly proportional to the *dc* photocurrent. In order to characterise the shot noise power in a typical room the induced *dc* current was measured for a set of different light conditions. The measurements of the induced current were made using a PIN photodiode with and without a optical high pass filter. The used PIN photodiode has: i) an active

area of $0.85cm^2$, ii) a parasitic capacitance of *120pF* (with a reverse voltage across the photodiode of *15V*), iii) a field of view of 85^o, and iv) a responsitivity of *0.6A/W* at a centre wavelength of *850nm*.

The measurement setup was located at desk height in a room of *7.2m*×*5.9m* having a ceiling height of *3.1m*, and large windows placed at the west side. The experimental measurements were made during a clear sunny afternoon. The artificial light was composed by twelve *36W* fluorescent lamps which were switched on during some measurements. Table 1 presents the main results of the measured *dc* photocurrent.

PIN photodiode		**Light Conditions**			***dc* Photocurrent**	
Orientation	Position	Fluorescent Lamps	Incandescent lamp (60W) at 1m	Curtain	without any optical filter	with optical filter
aimed to ceiling	middle of the room	OFF	OFF	Closed	42μA	10.2μA
aimed to ceiling	middle of the room	ON	OFF	Closed	64μA	11.7μA
aimed to ceiling	middle of the room	OFF	ON	Closed	78μA	34.5μA
aimed to ceiling	middle of the room	ON	ON	Closed	100μA	35.5μA
aimed to ceiling	middle of the room	OFF	OFF	Open	65μA	14.5μA
aimed to ceiling	middle of the room	ON	OFF	Open	88μA	15μA
aimed to ceiling	middle of the room	OFF	ON	Open	102μA	38μA
aimed to ceiling	middle of the room	ON	ON	Open	124μA	39.5μA
aimed to ceiling	near the window	OFF	OFF	Closed	0.74mA	0.19mA
aimed to ceiling	near the window	OFF	OFF	Open	5.1mA	1.0mA
aimed to the sun	near the window	OFF	OFF	Open	10.2mA	4.1mA

Table 1. Measured photocurrent under different light conditions.

The measured values show that, even using a daylight filter, the induced *dc* current has a large dynamic range. The minimum value is about *10μA* and the maximum value is about *4mA*. The high dynamic range in the *dc* photocurrent has some impact on the system design, in particular on the design of the photodetector bias circuit.

A well designed front-end should have a bias resistance (R_b), defining the bias of the PIN photodiode, as large as possible minimising its thermal noise contribution. However, large values of the induced current may reduce the reverse voltage across the photodiode. This results in an increase of the PIN photodiode parasitic capacitance which reduces the front-end bandwidth and increases the f^2 noise which is proportional to the square of the capacitance. In dimensioning photodiode bias resistance we assumed that in a typical office environment the induced photocurrent could be as high as *1mA/photodiode*.

3. Encoding Method

The developed infrared transceivers use Differential Manchester line coding. In Manchester coding, each data bit is splitted in two *mid-bits* (two time slots) and, therefore, there is always a transition at the middle of each bit. A binary "1" is represented by a pulse in the right *mid-bit* and a binary "0" is represented by a pulse in the left *mid-bit*. In Differential Manchester coding, an integration operation is performed on the incoming data before Manchester encoding operation. An example of Differential Manchester coded data is shown in figure 2.

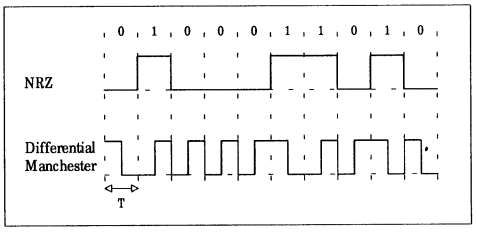

Figure 2. Differential Manchester coding vs. NRZ

This encoding method has a set of advantages: i) it has no *dc* component allowing low frequency rejection; ii) clock recovering is an easy operation; iii) encoder and decoder design is simple to implement. However, these advantages are achieved at the expense of a 50% code efficiency which results in a large bandwidth required.

III. The Optical Transceiver

1. The IR Emitter

A block diagram of the IR emitter is shown in figure 3. The transmission system operates at *1Mbps* using Differential Manchester line coding.

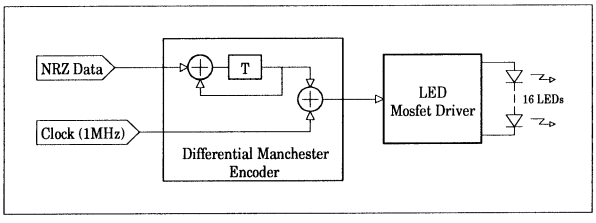

Figure 3. Block diagram of the IR emitter

The IR transmitter has two major blocks: a Differential Manchester encoder and a MOSFET driver circuit driving an array of 16 LEDs. The driver consists of a MOSFET transistor which drives the LEDs with a peak current of about *205mA*. It accepts a binary Differential Manchester signal and converts it into an optical signal. The IR transmitter emits an average optical power of about *400mW* with a centre wavelength of *850nm*. The optical pulse width is *500ns* with *18.2ns* risetime and *34ns* falltime.

The LEDs orientation was optimised in order to equalise the power distribution over the communication cell. A squared room with *9m*×*9m* and with a ceiling height of *3m* was considered in the optimisation of distributed power. The emitter radiation pattern was optimised using a simulation package developed by Lomba [7]. The optimised pattern was achieved following an approach similar to that presented in [9]. The optimised power distribution over the communication cell is presented in figure 4.

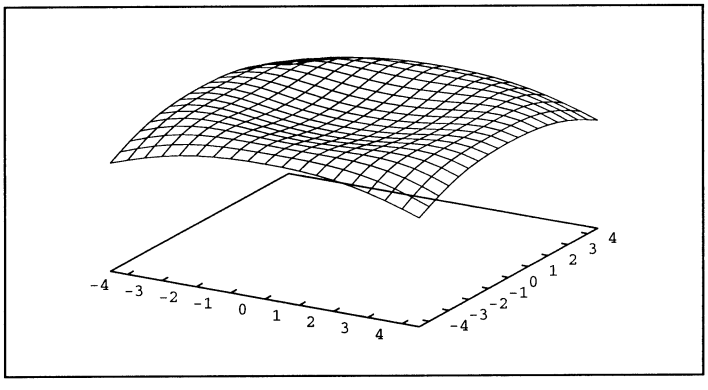

Figure 4. Optimised power distribution.

The simulation considered only the first order reflections on the room ceiling, which is a worst-case situation. In real environments higher order reflections will increase the received power.

During the optimisation procedure the transceiver was assumed vertically oriented and two types of LEDs were used. The LEDs characteristics were: A) P_t = *12mW*@50mA and *HPBW* = *15°* (*HPBW* - half power beam width); B) P_t = *15mW*@50mA and *HPBW* = *50°*.

The power distribution of figure 4 was achieved using two arrays of LEDs with the following orientation:

- *15* LEDs, type A, oriented at *58°* with the vertical and uniformly distributed on the azimuth plane.
- *1* LED, type B, oriented vertically.

Using this optimised array and for a total emitted power of *400mW*, the minimum and maximum irradiance values within the cell were $151nW/cm^2$ and $261nW/cm^2$, respectively.

2. The IR Receiver

A block diagram of the IR receiver is shown in figure 5. The IR receiver includes two arrays of PIN photodiodes, a differential low noise transimpedance amplifier, a comparator, a carrier sense circuit, a clock recovery circuit and a Differential Manchester decoder.

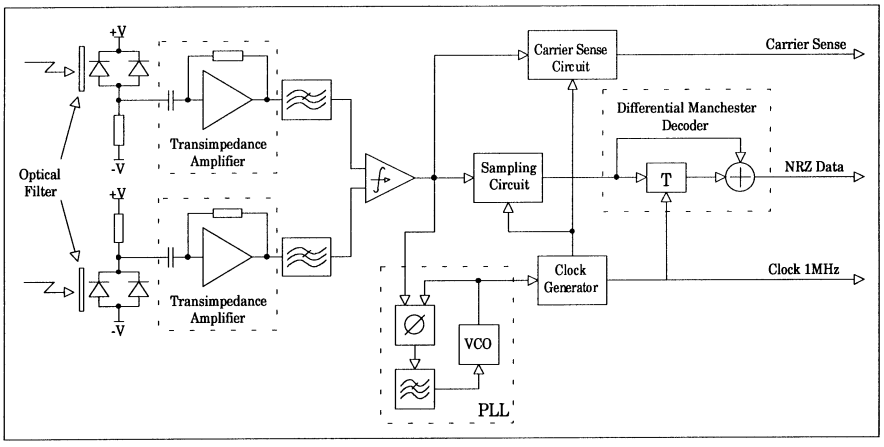

Figure 5. Block Diagram of experimental IR receiver.

An optical filter is used in front of the photodetector array in order to reduce the noise and interference induced by the ambient light. The measurements and characterisation of indoor illumination sources, presented in [10], shows that most of the optical interference are in the low frequency range except for fluorescent lamps. A capacitive coupling is placed at the receiver input to minimise low frequency interference as well as to avoid front-end saturation due *dc* photocurrent.

The photodetector array is composed by four photodiodes with a FOV of 85^o corresponding to a total active area of about $3.4cm^2$. This array presents a high capacitance to the front-end input limiting the receiver bandwidth. The IR receiver is splitted in two complementary low noise transimpedance amplifiers with a transimpedance gain of $470k\Omega$. This approach has two main objectives: i) to use differential circuits in order to reduce the penalty induced by electromagnetic interference (EMI); ii) to increase the receiver bandwidth avoiding equalisation. To improve the EMI immunity, the printed circuit board (PCB) layout was carefully designed with the two complementary front-ends identically implemented.

Following each complementary circuit a second order active low-pass filter is used. This active filter is an approximation to a raised cosine shaping filter to minimise the intersymbol interference (ISI). The complementary outputs of the active filters are compared resulting in a two level signal (TTL signal).

The carrier sense (CS) circuit implements a detection scheme based on the detection of Differential Manchester valid data. To enable CS signal, the CS circuit waits for a Differential Manchester valid pulse, and when it appears, it counts a precise number of valid pulses. The CS signal is disabled by the absence of transitions in the optical signal during two bit times.

A phase-locked loop (PLL) is used to recover the clock signal. A sampling circuit and a Differential Manchester decoder convert the encoded signal to NRZ.

IV. Theoretical Receiver Sensitivity

A theoretical model is presented to evaluate the receiver sensitivity. It includes the *dc* photocurrent induced by ambient light but it does not include the optical interference due artificial light. In the evaluation of the receiver sensitivity a *dc* photocurrent of $100\mu A/cm^2$ is considered. This value was achieved from table 1 and is assumed as a typical value in an indoor optical environment when daylight filters are used.

The use of two differential front-ends followed each one by a full raised cosine filter was included in the theoretical model. The differential IR receiver is composed by two identical transimpedance front-ends. Thus,

we will evaluate the receiver sensitivity of a simple transimpedance front-end and will extrapolate to the differential receiver front-end.

Case 1: Single front-end

In the evaluation of the receiver sensitivity we will use Personick's [11] optical receiver model. A basic transimpedance receiver is shown in figure 6.

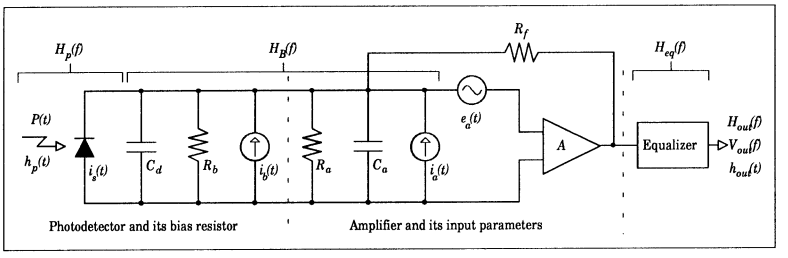

Figure 6. Schematic diagram of a typical optical receiver

The three main blocks of the optical receiver are the PIN photodiodes, the amplifier, and the equaliser. The photodiode has a capacitance C_d and a bias resistor R_b which generates a thermal noise current $i_b(t)$. The amplifier has an input impedance represented by the parallel combination of a resistance R_a and a shunt capacitance C_a. There are two amplifier noise sources: i) the input noise current source $i_a(t)$ which arises from the thermal noise of the amplifier input resistance R_a, and ii) the noise voltage source $e_a(t)$ which represents the thermal noise of the amplifier channel. The transimpedance amplifier has a feedback resistance R_f. The equaliser block is a raised cosine shaping filter.

The receiver sensitivity will be estimated as the minimum irradiance at the receiver level corresponding to a 10^{-9} bit error rate (BER). Using the Personick's reference model, and based on the work previously done by Smith and Garret [12] the required energy per pulse (b_{on}) to achieve a maximum error rate probability characterised by Q is:

$$b_{on} = 2\,Q\,\sigma \tag{1}$$

where $Q \cong 6$ for an error probability (P_E) of 10^{-9} and

$$P_E = \frac{1}{2}\,erfc\left(\frac{Q}{\sqrt{2}}\right) \tag{2}$$

Following the work done by [12,13] and since

$$P_{avr} = \frac{b_{on}}{2\,T_b} \tag{3}$$

the minimum irradiance for a determined BER is

$$H_{min} = \frac{P_{avr}}{A_r} = \frac{Q}{T_b\,A_r}\,\sigma \tag{4}$$

$$H_{min} = Q\,\frac{q}{\Re\,T_b\,A_r}\left[\frac{I_b}{q}\,T_b\,I_2 + W\right]^{\frac{1}{2}} \quad [W/cm^2] \tag{5}$$

where q is the electron charge, $\Re$ is the photodiode responsitivity, A_r is the total active area, I_b is the induced photocurrent, T_b is the pulse duration time, and W is a dimensionless parameter called the thermal noise characteristic of the receiver and is given by

$$W = \frac{T_b}{q^2}\left[S_I + \frac{2\,k_B\,\theta}{R'_b} + \frac{S_E}{R'^2}\right]I_2 + \frac{(2\pi C)^2}{q^2 T_b}\,S_E I_3 \tag{6}$$

where k_B is Boltzmann's constant, θ is the absolute temperature, S_I is the spectral density of the input noise current source, S_E is the voltage noise spectral density, given by

$$S_I = \frac{2\,k_B\,\theta}{R_{in}} \quad [A^2/Hz] \tag{7}$$

$$S_E = \frac{2\,k_B\,\theta\,R_{in}}{\beta} \quad [V^2/Hz] \tag{8}$$

and

$$R'_b = \left(\frac{1}{R_b} + \frac{1}{R_f}\right)^{-1} \tag{9}$$

$$R' = \left(\frac{1}{R_a} + \frac{1}{R_b} + \frac{1}{R_f}\right)^{-1} \tag{10}$$

$$C = C_a + C_d \tag{11}$$

I_2 and I_3 are the Personick's integrals, given by

$$I_2 = \frac{1}{T_b}\int_{-\infty}^{\infty}\left|\frac{H_{out}(f)}{H_p(f)}\right|^2 df = \int_{-\infty}^{\infty}\left|\frac{H'_{out}(\phi)}{H'_p(\phi)}\right|^2 d\phi \tag{12}$$

$$I_3 = T_b\int_{-\infty}^{\infty}\left|\frac{H_{out}(f)}{H_p(f)}\right|^2 f^2 df = \int_{-\infty}^{\infty}\left|\frac{H'_{out}(\phi)}{H'_p(\phi)}\right|^2 \phi^2 d\phi \tag{13}$$

Assuming $h_p(t)$ are rectangular input pulses and $h_{out}(t)$ are full raised cosine output pulses, the Personick's integrals I_2 and I_3 are respectively *1.127* and *0.174*.

The theoretical receiver sensitivity evaluation is made with the component values used in the prototype. These values are shown in table 2.

Parameter	Value
Input resistance of the first transistor	R_{in} = 1kΩ
PINs polarisation resistance	R_b = 10kΩ
Input resistance of the amplifier	R_a = 1kΩ
Feedback resistance	R_f = 560kΩ
Input capacitance of the amplifier	C_a = 10pF
Current gain of the first transistor	β = 200
PINs active area	A_r = variable
PINs parasitic capacitance	C_d = 120pF/cm^2
PINs responsitivity	ℜ = 0.6

Table 2. Values of optical receiver components.

Considering a photodetector active area of *3.4cm*^{2} (resulting in I_b = *3.4*100*μ*A* and *C = 3.4*120pF*) and using the preceding assumptions, the resulting receiver sensitivity (minimum irradiance) is H_{min} = *35.3nW/cm*^{2} (*-44.52dBm/cm*^{2}).

Case 2: Differential front-end

The evaluation of the differential receiver sensitivity is based on the above analysis. Figure 7 shows a simplified differential IR receiver which helps to understand the sensitivity evaluation.

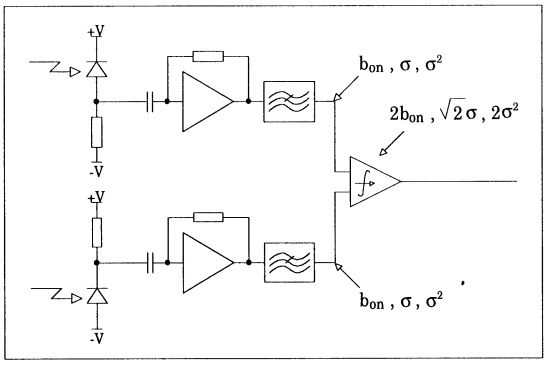

Figure 7. Simplified differential IR receiver.

The differential IR receiver is analysed as two single IR receivers with an active area of $A_r/2$ each one. With the two receivers associated in a differential mode, equation (1) turns into

$$2\, b_{on} = 2\, Q\sqrt{2}\,\sigma \tag{14}$$

Using the previous considerations, the minimum irradiance is

$$H_{min} = \frac{P_{avr}}{A_r/2} = \frac{\sqrt{2}Q}{T_b A_r}\sigma \tag{15}$$

with $Q \cong 6$.

Considering a photodetector active area of $3.4cm^2$ (resulting in $I_b = 1.7*100\mu A$ and $C = 1.7*120pF$ for each optical receiver) and using the preceding assumptions, the resulting differential receiver sensitivity is $H_{min} = 37.7nW/cm^2$ $(-44.23dBm/cm^2)$.

The penalty introduced by the differential receiver configuration is $0.29dB$. However, since our previous work demonstrated that high sensitivity optical receivers were too much sensitive to EMI we adopted a differential receiver configuration. The utilisation of a differential receiver turns the receiver sensitivity much less sensitive to EMI.

Figure 8 illustrates the calculated sensitivity, in terms of the required irradiance, versus photodetector active area. This curve corresponds to the differential receiver.

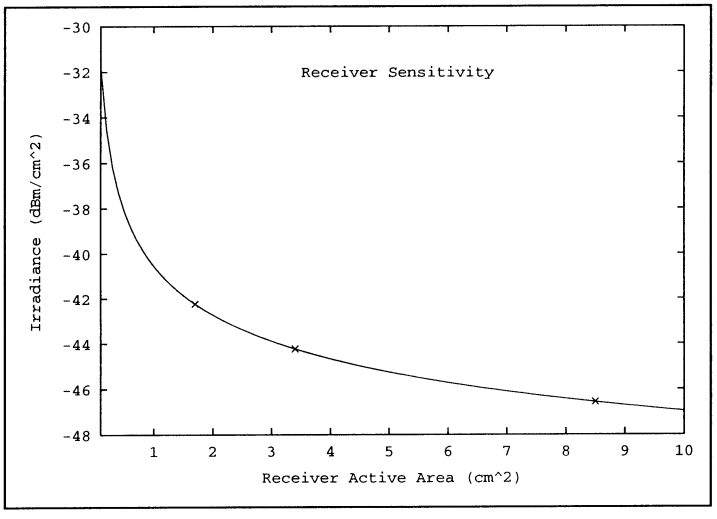

Figure 8. Receiver Sensitivity.

From figure 8, it can be seen that increasing the active area from $1.7cm^2$ to $8.5cm^2$ (corresponding to the utilisation of 2 and 10 PIN photodiodes, respectively), the receiver sensitivity is improved by about $4.4dB$. The high cost of large area PIN photodiodes leaves us to adopt a compromise between required sensitivity and global system cost. Thus, the adopted solution is to use 4 PIN photodiodes corresponding to a photodetector active area of about $3.4cm^2$. The penalty introduced by using 4 instead of 10 PIN photodiodes is about $2.4dB$ which is an acceptable value considering the reduction of the system cost.

V. Experimental Results

System operation was characterised in a typical room ($10m \times 6.2m$) with several tables and having a ceiling height of $3.1m$, and large windows located at the east and north side. The artificial light was created by sixteen $36W$ fluorescent lamps. The experimental measurements were made during Spring clear days. The IR transceivers were $0.8m$ above floor and vertically oriented. Table 3 presents the experimental measurements and compares them with the receiver sensitivity theoretically achieved. These experimental results were extended to different active areas ($1.7cm^2$, $3.4cm^2$ and $8.5cm^2$) and considering two different light conditions (1. natural light; 2. natural + fluorescent light).

Number of PIN photodiodes	Active Area (cm^2)	Sensitivity		
		Theoretical Value	Measured (Natural Light)	Measured (Natural + Fluorescent Light)
10	8.5	22nW/cm^2 -46.6dBm/cm^2 ( ) <> I_b = 100μA/cm^2	35nW/cm^2 -44.56dBm/cm^2 ( ) <+2.04dB> I_b = 70..80μA/cm^2	190nW/cm^2 -37.21dBm/cm^2 ( ) <+9.4dB> I_b = 80..95μA/cm^2
4	3.4	37.7nW/cm^2 -44.2dBm/cm^2 (+2.4dB) <> I_b = 100μA/cm^2	49nW/cm^2 -43.1dBm/cm^2 (+1.46dB) <+1.1dB> I_b = 35..45μA/cm^2	221nW/cm^2 -36.56dBm/cm^2 (+0.65dB) <+7.64dB> I_b = 65..80μA/cm^2
2	1.7	59.7nW/cm^2 -42.2dBm/cm^2 (+4.4dB) <> I_b = 100μA/cm^2	74nW/cm^2 -41.3dBm/cm^2 (3.26dB) <0.9dB> I_b = 35..60μA/cm^2	221nW/cm^2 -36.56dBm/cm^2 (+0.65dB) <+5.64dB> I_b = 70..95μA/cm^2

Note: ( ) - Penalty due to the reduction of the receiver active area (compared to the 10PINs situation).
<> - Penalty introduced by the ambient light conditions compared to the theoretical sensitivity.

Table 3. Receiver sensitivity of the IR receiver.

The results of table 3 show that under natural light conditions the achieved gain by using a large photodetector active area (*8.5cm²*) was *3.26dB* while the theoretical gain was *4.4dB*. Under these light conditions, the measured sensitivity is *2.04dB* distant from the theoretical value in the case of a *8.5cm²* photodetector active area. Using a small active area (*1.7cm²*), the difference between the measured sensitivity and the theoretical value is about *0.9dB* while for a photodetector active area of *3.4cm²* this difference is about *1.1dB*. These results show that the difference between theoretical and measured sensitivity increases with the increasing of photodetector active area. This phenomena is explained by the EMI which is not included in the theoretical sensitivity calculation. The utilisation of larger photodetector active areas implies more PIN photodiodes which work as "radio-frequency antennas" outside the receiver shielding.

Under natural and fluorescent light conditions there are no significant advantages to use a photodetector active area of *8.5cm²* instead of *1.7cm²* (*0.65dB*). Also, the measured sensitivity is far away from the theoretical values. We noticed that EMI induced by fluorescent lamps was very strong. In fact, fluorescent lamps are sources of radiofrequency interference with a large spectrum from about *100kHz* to *3MHz* [14]. Moreover, it must be noted that EMI and optical interference induced by fluorescent lamps are not included in the evaluation of the receiver sensitivity and Moreira [10] presented some results which demonstrate that the optical interference of fluorescent lamps geared by electronic ballasts are very large and have a wide spectrum up to *1MHz*. These two classes of interference (optical and radiated EMI) and the high sensitive receiver explain the difference when comparing measured and theoretical sensitivity. During our experiments we observed that the optical interference induced by fluorescent lamps dominates over EMI.

Figure 9 presents the theoretical and measured BER versus average received irradiance for the differential IR receiver with an active area of *3.4cm²*. The difference between the plotted results and the values shown in table 3 are explained by different ambient light conditions. These measurements were realised with an induced photocurrent varying from about *80μA/cm²* to about *140μA/cm²*.

Figure 9 shows that under natural light conditions there is a penalty of about *1.6dB* between the theoretical sensitivity and the experimental results. The penalty introduced by switching on the fluorescent lamps is about *6dB* relatively to theoretical sensitivity. The penalty introduced by fluorescent lamps, when compared to measured sensitivity under natural light conditions, is about *4.4dB*. In [10], it was studied the interference generated by fluorescent lamps and it was proposed a model to be used in the evaluation of the theoretical sensitivity.

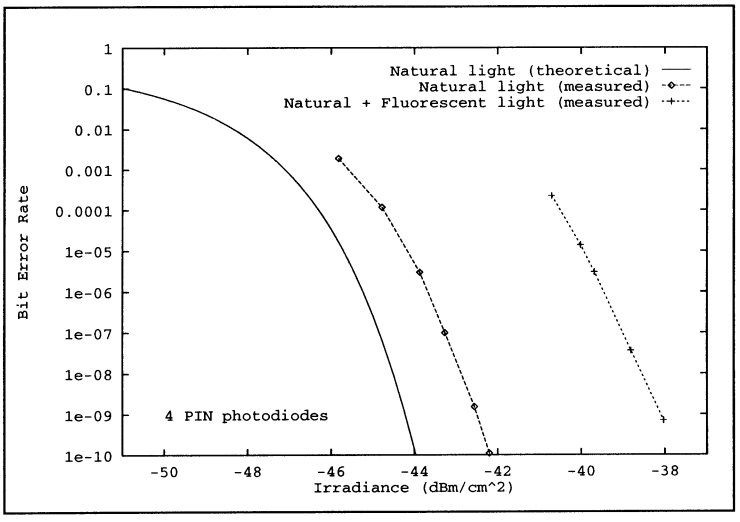

Figure 9. BER versus average received irradiance.

VI. Tests in an indoor WLAN environment

A WLAN environment using the implemented IR transceivers was setup and is shown in figure 10. The setup test is composed by two PCs, two Ethernet Adapters and two IR transceivers.

The setup test includes a block denominated Ethernet Adapter which implements the interface between an IR transceiver (*1Mbps*) and a BNC interface (*10Mbps*) of an Ethernet Network Interface Card. The Ethernet Adapter stores data and sends frames at the adequate bit rates. It integrates also the BNC interface and the IR transceiver interface functions.

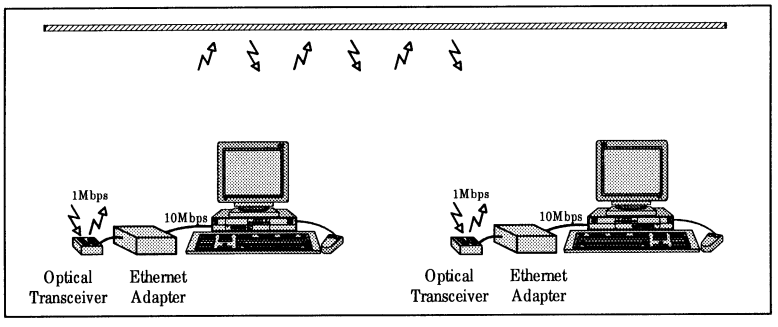

Figure 10. WLAN environment used to test IR transceivers.

During the experimental tests, one of the PCs was used as FTP server. FTP sessions were opened remotely by the second PC. After the establishment of the FTP session some FTP capabilities were used (file transfer and remote disk access). The packet length, used during FTP sessions, was configured to 1024 bytes.

The system was tested in the room described in section V with all fluorescent lamps switched on. Under these conditions, the FTP session was successfully established and some of its used capabilities worked properly with the IR transceivers over an horizontal distance of about *7m* between the two stations. The achieved throughput was about *400kbps* which is approximately ten times lower than a good throughput normally achieved in Ethernet.

VII. Conclusions

The feasibility of a diffuse IR WLAN using Differential Manchester line coding at a *1Mbps* data rate was demonstrated. The implemented optical transceivers worked properly in a communication cell of about *7m* diameter with a large amount of optical noise (natural and fluorescent light).

We have presented a model for the theoretical sensitivity of a differential optical receiver derived from Personick's model. The measurements are close to theoretical predictions only when natural light conditions are presented. It was shown that the optical interference and the EMI induced by fluorescent lamps introduce a large penalty in the receiver sensitivity. This means that the theoretical model should be reviewed to consider the interference induced by fluorescent lamps.

The design of high sensitive optical receivers will require careful attention on the topology. It was demonstrated that a differential topology attenuates the EMI induced in the layout of the optical receiver.

Acknowledgements

The first author would like to thank to JNICT (*Junta Nacional de Investigação Científica e Tecnológica*) for its financial support through a *Ph.D.* grant BD/2599/93. This work was partially funded by the European Commission via project ESPRIT.6892 POWER (*Portable Workstation for Education in Europe*).

References

[1] F. R. Gfeller, U. Bapst, "Wireless In-House Data Communication via Diffuse Infrared Radiation", Proceedings of the IEEE, Vol. 67, No. 11, Nov. 1979.

[2] J. R. Barry, J. M. Hahn, E. A. Lee, D. G. Messerschmitt, "High-Speed Nondirective Optical Communication for Wireless Networks", IEEE Network Magazine, pp. 44-54, Nov. 1991.

[3] R. T. Valadas, A. M. O. Duarte, "Sectored Receivers for Indoor Wireless Optical Communication Systems", PIMRC'94, *IEEE International Symposium on Personal, Indoor and Mobile Radio Communications*, pp. 1090-1095, The Hague, Netherlands, Sep. 18-23, 1994.

[4] A. J. C. Moreira, R. T. Valadas, A. M. O. Duarte, "Design and Implementation Issues of a Wireless Infrared Ethernet Link", PIMRC'92, *The Third IEEE International Symposium on Personal, Indoor and Mobile Radio Communications*, Boston, Massachusetts, Oct. 19-21, 1992.

[5] P. P. Smyth, M. McCullagh, D. Wisely, D. Wood, S. Ritchie, P. Eardley, S. Cassidy, "Optical wireless local area networks - enabling technologies", BT Technological Journal, Vol. 11, No. 2, Apr. 1993.

[6] C. J. Georgopoulos, S. H. Soultanidis, "Design of Manchester-PCM/demodulation circuitry for in-house wireless infrared communication system", International Journal of Optoelectronics, Vol. 8, No. 1, pp. 39-48, 1993.

[7] C. R. A. T. Lomba, R. T. Valadas, A. M. O. Duarte, "Propagation Losses and Indoor Optical Channel: A Simulation Package", In *International Zurich Seminar on Digital Communications*, pp. 285-297, Zurich, Switzerland, Mar. 8-11, 1994. Springer-Verlag.

[8] T.-H. Tsaur, K.-C. Chen, C. Lien, M.-T. Shih, C. P. J. Tzeng, "A Nondirective Infrared Transceiver for Indoor High Speed Wireless Data Communication", IEEE Transactions on Consumer Electronics, Vol. 40, No. 1, Feb. 1994.

[9] C. R. A. T. Lomba, R. T. Valadas, A. M. O. Duarte, "Flexible Emitter Radiation Pattern for Indoor Wireless Local Area Networks", COMCON V, *International Conference on Advances in Communication & Control*, Crete, Greece, Jun. 26-30, 1995.

[10] A. J. C. Moreira, R. T. Valadas, A. M. O. Duarte, "Artificial Light Interference in Wireless Infrared Transmission Systems", to be presented at PIMRC'95, *The Sixth IEEE International Symposium on Personal, Indoor and Mobile Radio Communications*, Toronto, Canada, Sep. 27-29, 1995.

[11] S. D. Personick, "Receiver Design for Digital Fiber Optic Communication Systems, I", The Bell System Technical Journal, Jul.-Aug., 1973.

[12] D. R. Smith, I. Garret, "A simplified approach to digital optical receiver design", Optical and Quantum Electronics 10, pp. 211-221, 1978.

[13] G. Keiser, "Optical Fiber Communications", McGraw-Hill, 1983.

[14] Keiser, B., "Principles of Electromagnetic Compatibility", 3rd edition, Artech House, 1987.